Journal of Molecular Liquids 350 (2022) 118550

Contents lists available at ScienceDirect

Journal of Molecular Liquids

journal homepage: www.elsevier.com/locate/molliq

Improvement of the lubrication performance of an ester base oil with coated ferrite nanoadditives for different material pairs

María J.G. Guimarey [a,b,*], José M. Liñeira del Río [a], Josefa Fernández [a]

[a] Laboratory of Thermophysical and Tribological Properties, Nafomat Group, Department of Applied Physics, Faculty of Physics and Institute of Materials (iMATUS), University of Santiago de Compostela, 15782 Santiago de Compostela, Spain
[b] Department of Design and Engineering, Faculty of Science & Technology, Bournemouth University, Talbot Campus, Poole BH12 5BB, United Kingdom

ARTICLE INFO

Article history:
Received 3 December 2021
Revised 2 January 2022
Accepted 14 January 2022
Available online 19 January 2022

Keywords:
Lubricant
Nanoparticles
Nanoparticle coating
Material pairs
Tribological mechanisms
Wetting

ABSTRACT

In the present work, lubrication properties (friction and wear) of a synthetic ester oil, tris(2-ethylhexyl) trimellitate (TOTM) containing ferrite nanoparticles coated with oleic acid (F_3O_4-OA) were investigated for two different material pairs: steel ball-steel disc and silicon nitride ball-steel disc. Thus, four TOTM nanolubricants were formulated: TOTM + 0.010 wt% Fe_3O_4-OA, TOTM + 0.015 wt% Fe_3O_4-OA, TOTM + 0.020 wt% Fe_3O_4-OA and TOTM + 0.025 wt% Fe_3O_4-OA showing all of them a moderate time stability due to the oleic acid coating. Wettability behaviour of the ferrite-based nanolubricants on steel surface was analysed, revealing that the addition of Fe_3O_4-OA nanoparticles in TOTM decreases the contact angle between the steel surface and TOTM lubricant surface. Friction sliding tests were performed with the neat TOTM and with the formulated nanolubricants under a 20 N of load. All nanolubricants showed lower coefficients of friction than those reached with TOTM base oil for both material pairs. Worn area was significantly reduced for all Fe_3O_4-OA concentrations in the steel-steel contact and for the highest concentrations in the silicon nitride-steel contact. Specifically, the largest achieved reductions were for the TOTM + 0.010 wt% F_3O_4-OA nanolubricant: 43% reduction in friction (silicon nitride-steel) and reductions of 17% in wear track width, 42% in wear track deep and 36% in area (steel-steel). In addition, roughness analysis and Raman microscopy of the tested discs showed that tribofilm formation and surface repairing mechanisms occur.

© 2022 The Authors. Published by Elsevier B.V. This is an open access article under the CC BY-NC-ND license (http://creativecommons.org/licenses/by-nc-nd/4.0/).

1. Introduction

Lubricants are broadly used to reduce equipment friction and wear, thus increasing the service life of machines, particularly in environments with heavy contact loads [1,2]. Around 30% of energy consumption in machines is associated to mechanical friction and most of the mechanical failures are consequence from wear [3]. Furthermore, the wetting behaviour of lubricated flat surfaces could be strongly correlated with the tribological properties of a solid/lubricant pair [4]. To minimize friction and wear in systems, small amounts of additives are included to lubricant bases to improve their performance. It should be noted that conventional additives are chlorine or phosphorus materials that were limited in terms of use owing to the purpose of environment protection. To overcome this problem, nowadays some researchers are examining the use of nanoparticles (NPs) as a novel type of lubricant additive [5,6]. Furthermore, NPs are usually environmentally friendly and lead to tribological improvements of lubricants because they do not need tribo-active chemical elements such as chlorine, phosphorus, and sulphur that are harmful to environment [7]. In fact, much research shows that small amounts of NPs as lubricant additives have promising effects in reducing friction and wear [8–12]. Despite the advances made in NPs as lubricants additives, there is still a great limitation with stability of the nanolubricants since NPs tend to agglomerate and sediment [13]. Taking this fact into account, many researchers use dispersants to increase the nanolubricant stability [14,15]. However, better stabilities can be found when surface of the NPs is modified by a reaction with a surfactant [13]. The NPs obtained with this method are named as coated or functionalized NPs. Chen et al. [13] reviewed the stability times of many nanolubricants, analysing various characteristics of NPs such as their size and coating, concluding that surface modification of the NPs is critical to obtain nanolubricants with a good stability [16–20].

* Corresponding author at: Laboratory of Thermophysical and Tribological Properties, Nafomat Group, Department of Applied Physics, Faculty of Physics and Institute of Materials (iMATUS), University of Santiago de Compostela, 15782 Santiago de Compostela, Spain.
E-mail address: mariajesus.guimarey@usc.es (M.J.G. Guimarey).

https://doi.org/10.1016/j.molliq.2022.118550
0167-7322/© 2022 The Authors. Published by Elsevier B.V.
This is an open access article under the CC BY-NC-ND license (http://creativecommons.org/licenses/by-nc-nd/4.0/).

Carbon- and metallic-based nanomaterials are the most used NPs in tribological applications [8,21–23]. In particular, metal magnetic NPs are generally investigated due to their many applications such as drug-delivery, magnetic records as well as additives of lubricants being anti-wear enhancers [20,24]. In the latter field, several authors investigated the use NPs of iron oxides as lubricant additives with good tribological properties. Thus, Liñeira del Río et al. [20] measured the anti-friction and anti-wear properties of Fe_3O_4 NPs coated with oleic acid as additives of trimethylolpropane trioleate finding friction reductions up to 18% and wear reductions up to 59%. In addition, Hu et al. [25] studied the tribological behaviour of uncoated ferric oxide (Fe_2O_3) NPs as a lubricant additive of SN500 mineral oil, observing a wear improvement of 12% in comparison with neat SN500 oil. Furthermore, Zhou et al. [24] studied the tribological performance of Fe_3O_4 magnetic NPs with an oleic acid coating as liquid paraffin additives, achieving friction and wear reductions of 25% and 65%, respectively.

The main goal of this work is to analyse the tribological performance in two different tribological contacts, steel-steel and silicon nitride-steel, of nanolubricants formed by magnetic ferrite NPs, Fe_3O_4, coated with oleic acid and tris(2-ethylhexyl) trimellitate (TOTM). This synthetic base oil is interesting as a lubricant due to its suitable properties: low vapour pressure, medium viscosities (88 cSt a 40 °C) and because it is liquid in a wide temperature range [26–29]. At atmospheric pressure the freezing and boiling temperatures are 230 and 687 K, respectively [29]. According to its material safety data sheet (MSDS) and European Directive 67/548/EEC, TOTM is classified as a non-hazardous substance [29]. Trimellitates are used in reciprocating compressors oils, high temperature chain lubricants, transformer fluids, textile lubricants as well as for the disk drive industry and high-temperature conveyor bearings [30]. Regarding the different tribo-pairs, it is interesting to analyse the tribological behaviour with different materials since the advanced ceramic elements usually show enhanced performances in comparison to the usual steel elements [31,32]. Up to our knowledge, there are no previous studies about tribological properties of functionalized nanoadditives of lubricants comparing two different tribological contacts.

2. Materials and methods

2.1. Materials

Tris(2-ethylhexyl) trimellitate, TOTM, (CAS Number: 3319-31-1) is a synthetic ester base oil supplied by Sigma-Aldrich (lot number: MKBT5164V) with a molecular weight of 546.789 g mol^{-1} and a purity mole fraction higher than 0.99. Dynamic viscosity at 313.15 K and viscosity index (VI) for the TOTM is 85.76 mPa s and 89, respectively [27]. A sample of TOTM was fully characterized through different techniques. Fig. 1 shows the infrared spectroscopy (FTIR) spectrum of TOTM, it can be observed the presence of a strong peak at 1724 cm^{-1}, associated to the stretching carbonyl vibration (—C═O), a peak at 1230 cm^{-1} that is attributed to (—C—O—C) single bond stretching vibration and peaks around 2930 cm^{-1} which correspond to carbon–hydrogen (—CH_2, —CH_3) stretching [33,34].

Raman spectrum of the base oil was recorded using a WITec alpha300R+ confocal microscope with a laser beam of wavelength 532 nm. As can be observed in Fig. 2, a broad Raman band around 2800–3000 cm^{-1} is detected with three peaks at 2845, 2874 and 2911 cm^{-1} associated with C—H stretching vibrations [35]. Other intense peaks can be seen at 1729 and 1608 cm^{-1} corresponding to C═O stretching mode and ring-skeletal stretching, respectively. Additional peaks at 1457, 1404 and 1260 cm^{-1} can be assigned to CH_3 asymmetric deformation, CH_3 symmetric deformation and C—O—C stretching deformation, respectively [35].

Ferrite NPs coated with oleic acid (Fe_3O_4-OA) of 6.3 nm average size were kindly provided by the NANOMAG research group (University of Santiago de Compostela). A description of the synthesis process and further characterisation of these nanomaterials were previously published [20].

2.2. Nanolubricants formulation and stability

The nanolubricants were prepared by a two-step method, first using a Sartorius MC210P high-precision balance to weigh the appropriate amount of nanoadditives and base oil, followed by the use of a Fisherbrand ultrasonic bath to sonicate the dispersions

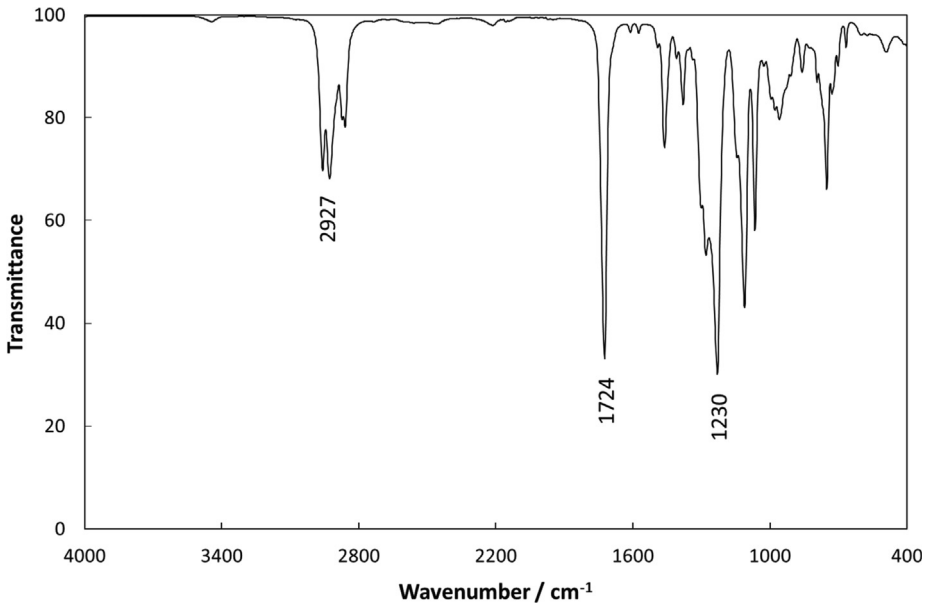

Fig. 1. FTIR spectrum of Tris(2-ethylhexyl) trimellitate base oil.

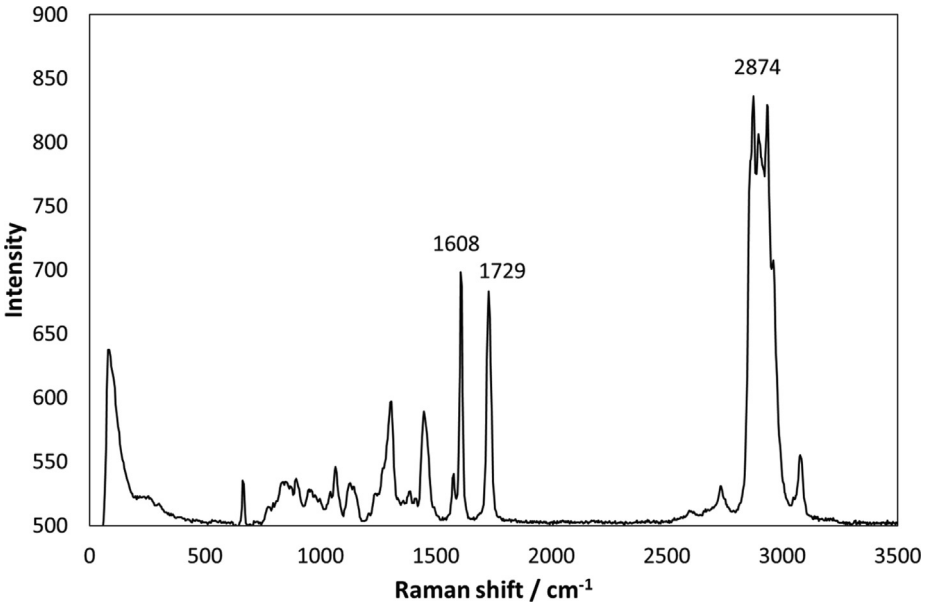

Fig. 2. Raman spectrum of Tris(2-ethylhexyl) trimellitate, TOTM, base oil.

Table 1
Specimen properties.

Specimen	Lower: Disc	Upper: Ball 1	Upper: Ball 2
Material	AISI 52100/535A99 steel	AISI 52100/535A99 steel	Silicon-nitride ceramic
Radius/mm	5	3	3
Hardness	Vickers scale 190–210 Hv30	Rockwell Scale 58–66	Rockwell Scale 75–80
Roughness/μm	0.02	<0.05	<0.05

with continuous stirring periods of 4 h and at 37 kHz of frequency. The nanolubricant concentrations prepared were 0.010, 0.015, 0.020 and 0.025 wt% Fe_3O_4-OA in TOTM. These NPs loadings were selected as in previous work a better tribological performance was obtained when low concentrations of nanoadditives were used [20].

Once the nanolubricants were prepared, an evaluation of their stability was carried out. Two different methods have been used to evaluate the stability of the NPs in TOTM and to check whether sedimentation of the NPs occurs. These methods are visual control and time evaluation of the refractive index of the nanolubricants.

2.3. Contact angle measurements

The contact angles, θ, corresponding to the TOTM base oil and to the TOTM nanolubricant with the higher Fe_3O_4-OA content (0.025 wt%) were determined using an automated Phoenix MT(A) contact angle analyser in static mode at three temperatures: 293.15, 313.15 and 333.15 K. A thermostatic bath was coupled to the analyser to keep the sample at constant temperature with an uncertainty of ±0.1 K. Static contact angles were measured by the sessile drop method, depositing the test liquid on the surface using a motorized syringe device. AISI 52100 steel (surface roughness: 0.02 μm), widely used in bearing manufacture [36], was the material selected to study the wetting behaviour of the lubricants. An image of the advancing droplet was captured every second for an interval of 180 s, a time long enough for the droplet to reach a steady state. At least three measurements were repeated for each sample. The θ values were obtained with an expanded uncertainty of 1° (95 % confidence level).

2.4. Friction tests

Friction rotational tests were performed using a CSM Standard tribometer working in ball-on-disc configuration, for TOTM and the four formulated nanolubricants under the following conditions: 20 N load (1.8 and 2.0 GPa maximum contact pressure for steel-steel and silicon nitride-steel contacts, respectively), room temperature, 3 mm radius trajectory, 340 m distance and 0.10 $m{\cdot}s^{-1}$ sliding speed. The specifications of the different specimens used in this work are listed in Table 1. Prior to friction tests, balls and discs have been cleaned in an ultrasonic acetone bath with the aim of removing any residual material. Subsequently, each disc has been lubricated with about 0.15 mL of the lubricant under study, performing at least three replicates for each nanolubricant to ensure an appropriate repeatability. Once the friction tests have been carried out, the specimens are cleaned with hexane for the subsequent evaluation of the wear obtained. For this task, a 3D Optical Profiler (Sensofar S Neox) in confocal mode with a 10× objetive lens is used to measure the wear produced on the steel discs through different parameters such as: wear track width (WTW), wear track depth (WTD) as well as transversal worn area. It should be noted that these parameters were measured at three locations on each worn track to obtain suitable average values. Furthermore, this device is also used to determine the roughness (Ra) of the worn surfaces of steel discs used in friction tests to characterize the anti-wear capacity of each nanolubricant.

Finally, a Raman microscope (WITec alpha300R+) was used to examine the surface of the worn tracks of the steel discs and obtain information of the distribution of the NPs therein, as well as of the possible tribological mechanisms that occur. Raman spectra were obtained with a 532 nm wavelength laser.

3. Results and discussion

3.1. Nanolubricant stability

Fig. 3 shows the photographs taken for the nanolubricants of Fe_3O_4-OA NPs with concentrations from left to right side: 0.010, 0.015, 0.020 and 0.025 wt%. As can be observed in Fig. 3a, the nanolubricants at the time of preparation have a homogeneous appearance and the nanoadditives are perfectly dispersed in the base oil. During the two weeks in which this stability monitoring was carried out daily, no precipitation or visual agglomeration of the NPs was observed, as shown in Fig. 3b and 3c. However, at the end of this monitoring, the bottom of the vial was checked, and a slight precipitation was observed for the nanolubricant of highest concentrations (0.015, 0.020 and 0.025 wt%).

To complete the study of the stability of the nanolubricants, the temporal evolution of the refractive index was measured from the preparation of the samples up to 96 h (4 days) for the nanolubricant with the highest concentration (0.025 wt%) and that with

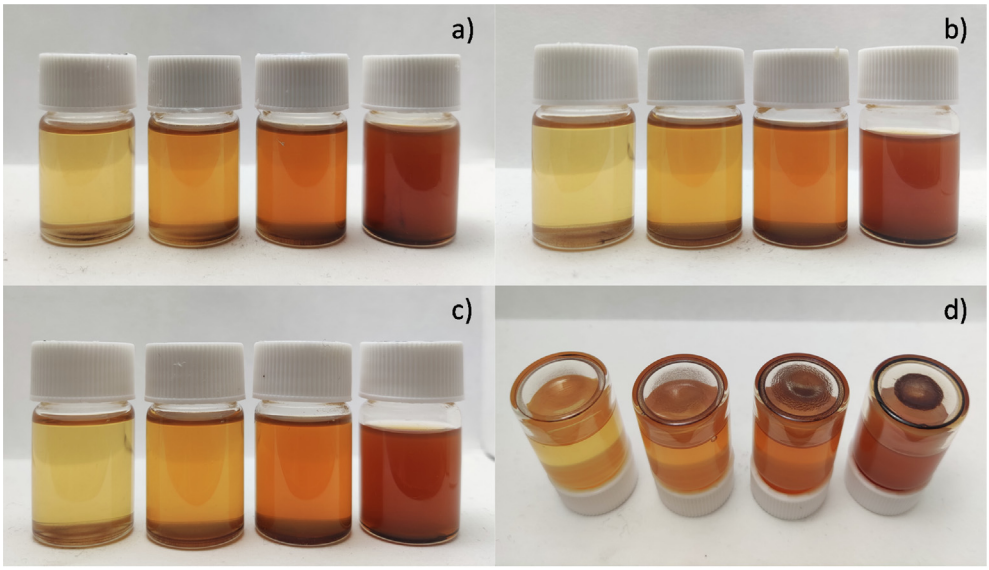

Fig. 3. Visual control of ferrite-based nanolubricants a) at the time of preparation, b) one week after preparation, c) and d) two weeks after preparation. From left to right side the concentration of the Fe_3O_4-OA NPs of the nanolubricants are 0.010, 0.015, 0.020 and 0.025 wt%

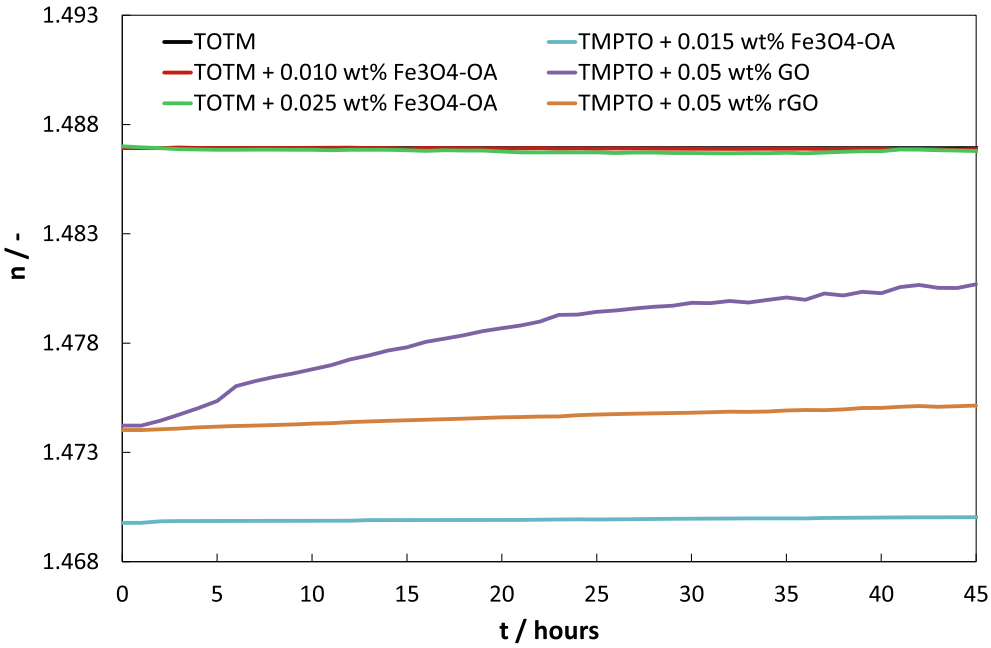

Fig. 4. Temporal evolution of refractive index, n, for the different TOTM- and TMPTO-based nanolubricants at 293.15 K.

the lowest concentration (0.010 wt%), as well as for the base oil, TOTM. Both nanolubricants show excellent stability since variations in the refractive index at 96 h of 0.008 and 0.011 %, with respect to the base oil (with a constant value of n = 1.48692), were observed for TOTM + 0.010 wt% Fe_3O_4-OA, and TOTM + 0.025 wt% Fe_3O_4-OA, respectively. As expected, the nanolubricant with the lowest concentration has slightly better stability. In Fig. 4, a comparison is shown between the stability of current nanolubricants and previously studied nanolubricants: TMPTO + 0.05 wt% GO, TMPTO + 0.05 wt% rGO and TMTPO + 0.015 wt% Fe_3O_4-OA [20]. For these nanolubricants the refractive index varies 0.44, 0.08 and 0.02 % after 45 h, respectively, whereas for TOTM + 0.010 wt % Fe_3O_4-OA, and TOTM + 0.025 wt% Fe_3O_4-OA the variations are 0.003 and 0.014 %. Thus, smaller variations are obtained with the TOTM-based nanolubricants, showing the good stability of the ferrite nanoparticles in TOTM lubricant due to the oleic acid coating.

3.2. Wetting behaviour

The wettability of a solid surface by a lubricant (liquid) can be characterized by the contact angle that is formed by the tangent at the point contact of the profile of the liquid droplet and the liquid-solid surface. The contact angles at different temperatures on AISI 52100 steel were determined both for the base oil, TOTM, and for the nanolubricant with the highest ferrite concentration (0.025 wt%), to know how the addition of nanoadditives affects

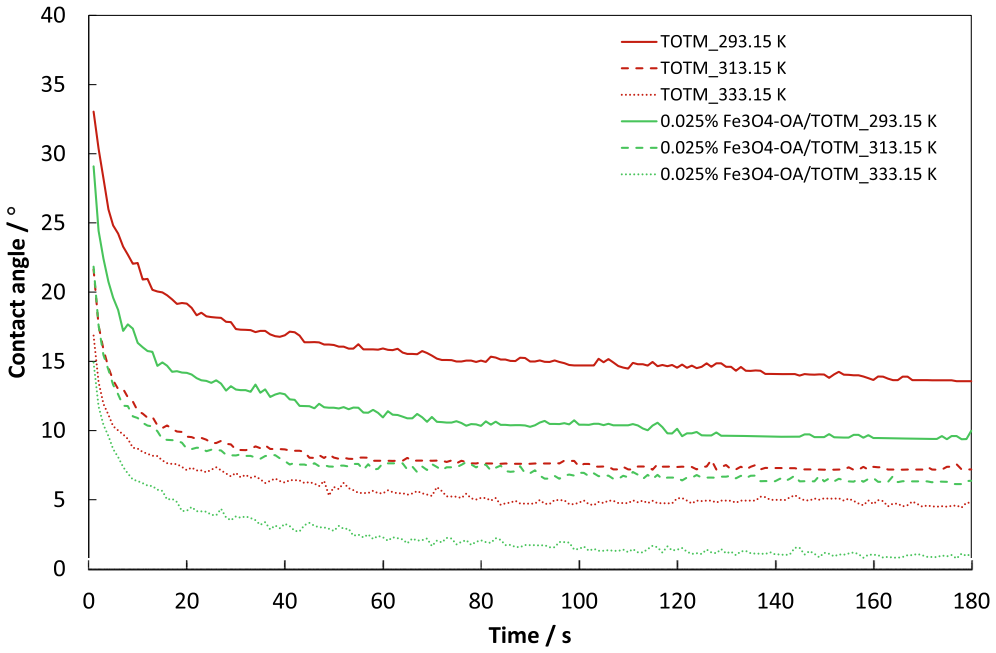

Fig. 5. Contact angle evolution of TOTM and of TOTM + 0.025 wt% Fe_3O_4-OA nanolubricant for 180 s at 293.15, 313.15 and 333.15 K.

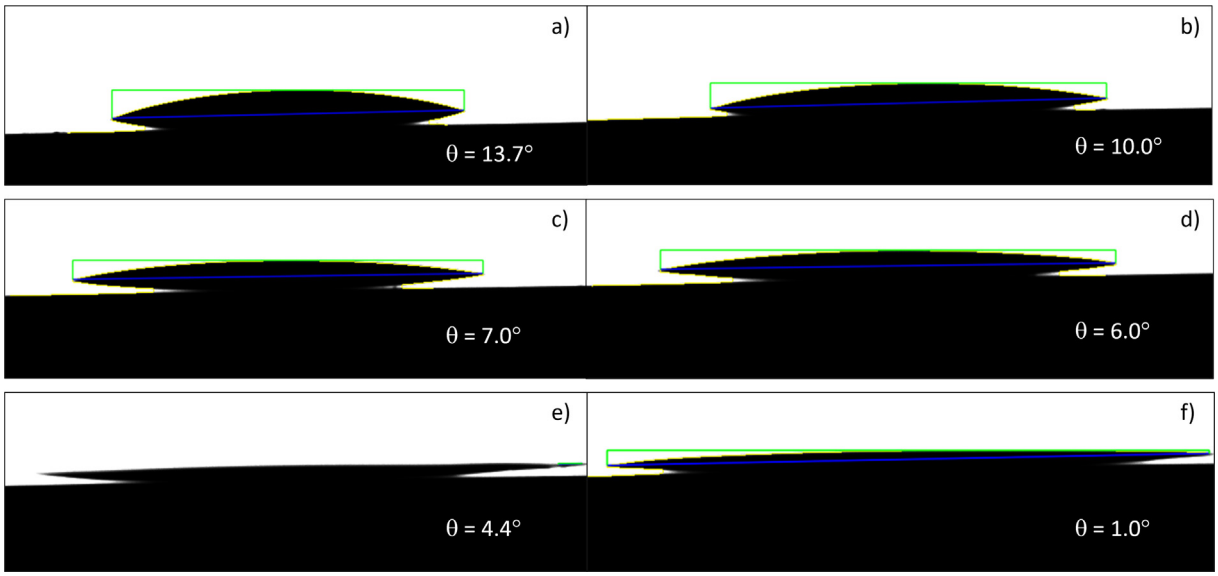

Fig. 6. Steady-state contact angle snapshots on AISI 52100 steel of a) TOTM at 293.15 K, b) TOTM + 0.025 wt% Fe_3O_4-OA at 293.15 K, c) TOTM at 313.15 K, d) TOTM + 0.025 wt % Fe_3O_4-OA at 313.15 K, e) TOTM at 333.15 K and f) TOTM + 0.025 wt% Fe_3O_4-OA at 333.15 K.

the wetting behaviour of the lubricant. Fig. 5 shows the advancing contact angle for 180 s, time at which steady state is assumed to be reached, for TOTM and for TOTM + 0.025 wt% Fe_3O_4-OA at 293.15, 313.15 and 333.15 K. A decrease in contact angle is observed with increasing temperature for both lubricants (with and without nanoadditive). While at the same temperature, a lower advancing contact angle is evident for the lubricant with the ferrite-based nanoadditives.

Fig. 6 gathers the steady state contact angle values for TOTM and nanolubricant at different temperatures. The wettability of this base oil is outstanding, but the wettability of its nanolubricants is even better (lower contact angle). Thus, it has been observed that the presence of the nanoadditive in the base oil causes a decrease in the steady-state contact angle for all temperatures studied, in concordance with the results of Fig. 5. For instance, at 293.15 K the steady-state contact angle for TOTM is 13.7°, while under the same conditions for nanolubricant it is 10.0°, as can be seen in Fig. 6. The smallest contact angle is obtained after an addition of 0.025 wt% Fe_3O_4-OA to the TOTM lubricant at 333.15 K. Hence, the distribution of Fe_3O_4-OA nanoparticles on the surface of the oil droplets improves the wetting behaviour of the oil. Some studies [37] have shown the relationship of the contact angle to the lubrication effect, as a lower contact angle results in better wettability at the lubricant-solid interface.

In a previous work [38], contact angle results for TOTM on AISI 420 stainless steel surface at 293.15, 303.15, 313.15 and 323.15 K at 5 s after drop fall have been reported. Comparing both experimental results, the contact angle value for TOTM is 24.8° (Fig. 5) and 21.9° [38] on surface of AISI52100 steel (100Cr6) and on stainless steel surface (AISI420), respectively, at a temperature of

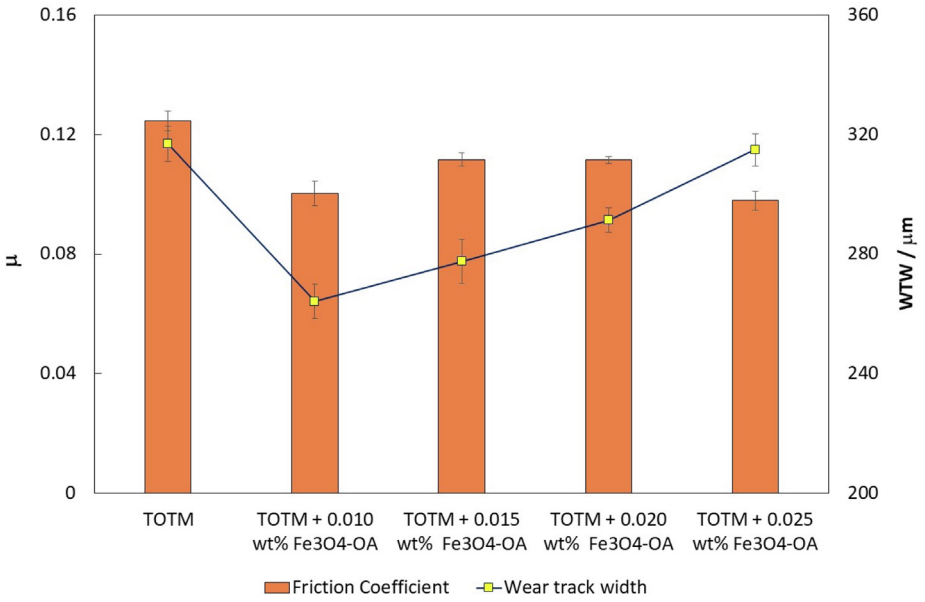

Fig. 7. Friction coefficients (μ) and wear track widths (WTW) on the steel discs obtained with TOTM nanolubricants for steel-steel contacts.

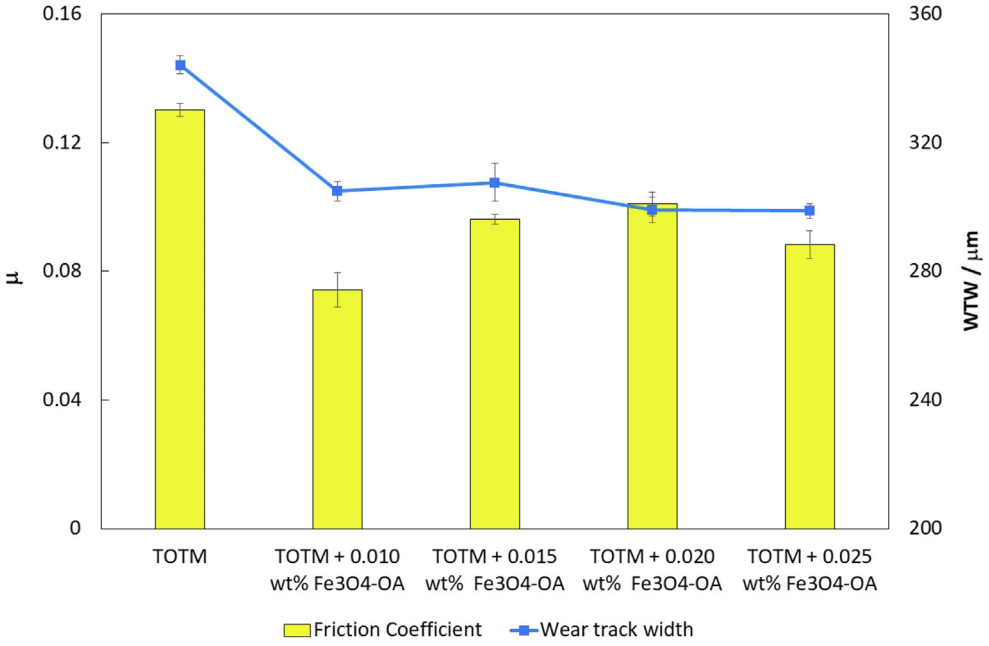

Fig. 8. Friction coefficients (μ) and wear track widths (WTW) on the steel discs obtained with TOTM nanolubricants for silicon nitride-steel contacts.

Table 2
Average friction coefficients (μ), wear track width (WTW), wear track depth (WTD), and area and their corresponding standard deviations (σ) for the lubricants in steel-steel contacts.

Lubricant	μ	σ	WTW/μm	σ/μm	WTD/μm	σ/μm	Area/10^2μm^2	σ/10^2μm^2
TOTM	0.1245	0.0033	316.9	5.9	4.25	0.37	6.06	0.60
+ 0.010 wt% Fe_3O_4-OA	0.1003	0.0041	264.2	5.7	2.48	0.20	3.89	0.46
+ 0.015 wt% Fe_3O_4-OA	0.1116	0.0021	277.6	7.3	2.88	0.21	4.19	0.50
+ 0.020 wt% Fe_3O_4-OA	0.1115	0.0012	291.3	4.1	2.84	0.20	4.54	0.38
+ 0.025 wt% Fe_3O_4-OA	0.0979	0.0032	314.9	5.4	2.69	0.25	4.12	0.29

Table 3
Average friction coefficients (μ), wear track width (WTW), wear track depth (WTD), and area and their corresponding standard deviations (σ) for the lubricants in silicon nitride-steel contacts.

Lubricant	μ	σ	WTW/μm	σ/μm	WTD/μm	σ/μm	Area/10^2μm^2	σ/10^2μm^2
TOTM	0.1302	0.0020	344.1	2.8	1.98	0.23	4.04	0.51
+ 0.010 wt% Fe_3O_4-OA	0.0743	0.0055	304.9	3.2	2.55	0.27	4.90	0.48
+ 0.015 wt% Fe_3O_4-OA	0.0963	0.0015	307.7	5.8	2.30	0.15	4.79	0.43
+ 0.020 wt% Fe_3O_4-OA	0.1009	0.0036	299.1	4.0	1.82	0.22	3.60	0.32
+ 0.025 wt% Fe_3O_4-OA	0.0883	0.0044	298.8	2.3	2.22	0.21	3.81	0.35

293.15 K and 5 s dwell time. This difference may be due to the different composition of the two steel substrates and their different surface roughness, 20 nm and 10 nm, respectively.

3.3. Tribological results

Mean coefficients of friction (μ) for TOTM base oil and for the designed TOTM nanolubricants between steel-steel and silicon nitride-steel tribological contacts are displayed in Fig. 7 and Fig. 8, respectively. It is worth mentioning that the silicon nitride-steel contact has a slightly higher friction coefficient (0.1302) than the steel-steel contact (0.1245) when lubricated with TOTM under the same conditions (Tables 2 and 3). The friction coefficient decreases for all nanolubricants compared to those of the neat TOTM oil, especially in the case of silicon nitride-steel contacts (Fig. 8). In particular, for steel-steel contacts the best anti-friction enhancement is obtained with the nanolubricant TOTM + 0.025 wt% F_3O_4-OA, showing a friction coefficient of 0.0979 against 0.1245 reached with the neat TOTM (Table 2). Therefore, this result translates into a 21% reduction in the friction produced by the neat TOTM. Regarding the silicon nitride-steel contacts, greater friction reductions were achieved, specifically the best friction improvement was found for the TOTM + 0.010 w t% F_3O_4-OA nanolubricant with a 43% reduction.

Regarding the wear produced on the steel discs in the friction experimental tests, Figs. 7 and 9a evidence that worn tracks lubricated with all the designed Fe_3O_4-OA nanolubricants are smaller than those found when the discs are lubricated with the neat TOTM oil for steel-steel contact. Besides, Table 3 confirms how the wear obtained in nanolubricant tests is much lower than that achieved with base oil for all the parameters analysed (WTW, WTD as well as area), especially for the last two, indicating this fact that nanoparticles have optimal anti-wear properties. Therefore, the greatest reductions of 17% in WTW, 42% in WTD and 36% in transversal area have been found for the TOTM + 0.010 wt% Fe_3O_4-OA nanolubricant. On the other hand, for silicon nitride-steel contacts, improvements in WTW produced in the steel discs have also been observed using all the nanolubricants compared to that obtained with TOTM oil. However, in this case there are not enhancements in the depth and wear area parameters using some nanolubricants as the differences are within the standard deviation of the measurements (Table 3). The largest reductions of 13% in WTW, 8% in WTD and 11% in area have been found for the TOTM + 0.020 wt% Fe_3O_4-OA nanolubricant. The 3D profiles of the wear tracks on the steel discs obtained lubricating the different contacts with the ferrite-based nanolubricants compared to that corresponding to TOTM clearly show that some nanolubricants reduce strongly the wear especially for the TOTM + 0.010 w t% Fe_3O_4-OA nanolubricant in steel-steel contact. It is worth noting that no clear trends have been observed between the tribological performance of nanolubricants and their nanoadditive content. This can be explained by the fact that the when the nanoparticle concentration is too high, nanoparticles tend to agglomerate [39]. Aggregation can explain the lower efficiency of nanolubricants with higher concentration of nanoparticles, since prevents particles from entering the contact area of working surfaces, and leads to unstable tribological performance [40].

Roughness (Ra) inside the worn track surfaces was also investigated to examine the anti-wear properties of the nanolubricants. Table 4 shows that the worn tracks of the steel discs lubricated with each of tested nanolubricants have lower roughness than those lubricated with neat TOTM for steel-steel and silicon nitride-steel contacts. In particular, Ra values of 420 nm and 89.5 nm were found in TOTM worn scars (steel-steel and silicon nitride-steel tests) whereas for the scars lubricated with TOTM + 0.010 wt% Fe_3O_4-OA (steel-steel) and with TOTM + 0.020 wt% Fe_3O_4-OA (silicon nitride-steel) nanolubricants the smallest Ra values (200 and 44 nm, respectively) were reached, which implies reductions in roughness of up to 52% and 51%. From Table 4 and Fig. 9, it can be clearly seen that when the upper sample is silicon nitride, the roughness of the worn surfaces is much lower. This fact may be due to the fact that silicon nitride balls are much harder than steel balls, and therefore exert a greater polishing effect on worn surfaces. Besides, silicon nitride balls produce slightly wider and shallower worn scars than steel balls.

Finally, to complete the wear analysis, a Raman mapping was carried out to obtain more information that allows discussing the possible anti-wear mechanisms of the nanoparticles that explain the improved behaviour of these nanolubricants. Fig. 10. shows the Raman mapping with the distribution of the nanoparticles within the wear scar of the steel discs used in the steel-steel and silicon nitride-steel tests with the TOTM + 0.025 wt% Fe_3O_4-OA lubricant. The corresponding spectra of the different compounds (TOTM, carbon and Fe_3O_4) detected are also plotted in Fig. 10. Raman spectrum of the TOTM (Fig. 2) allows to identify the characteristic peaks of the oil that have been found (orange colour) in the worn tracks lubricated with 0.025 wt% Fe_3O_4-OA nanolubricant for both contacts (Fig. 10). The same occurs with the ferrite nanopar-

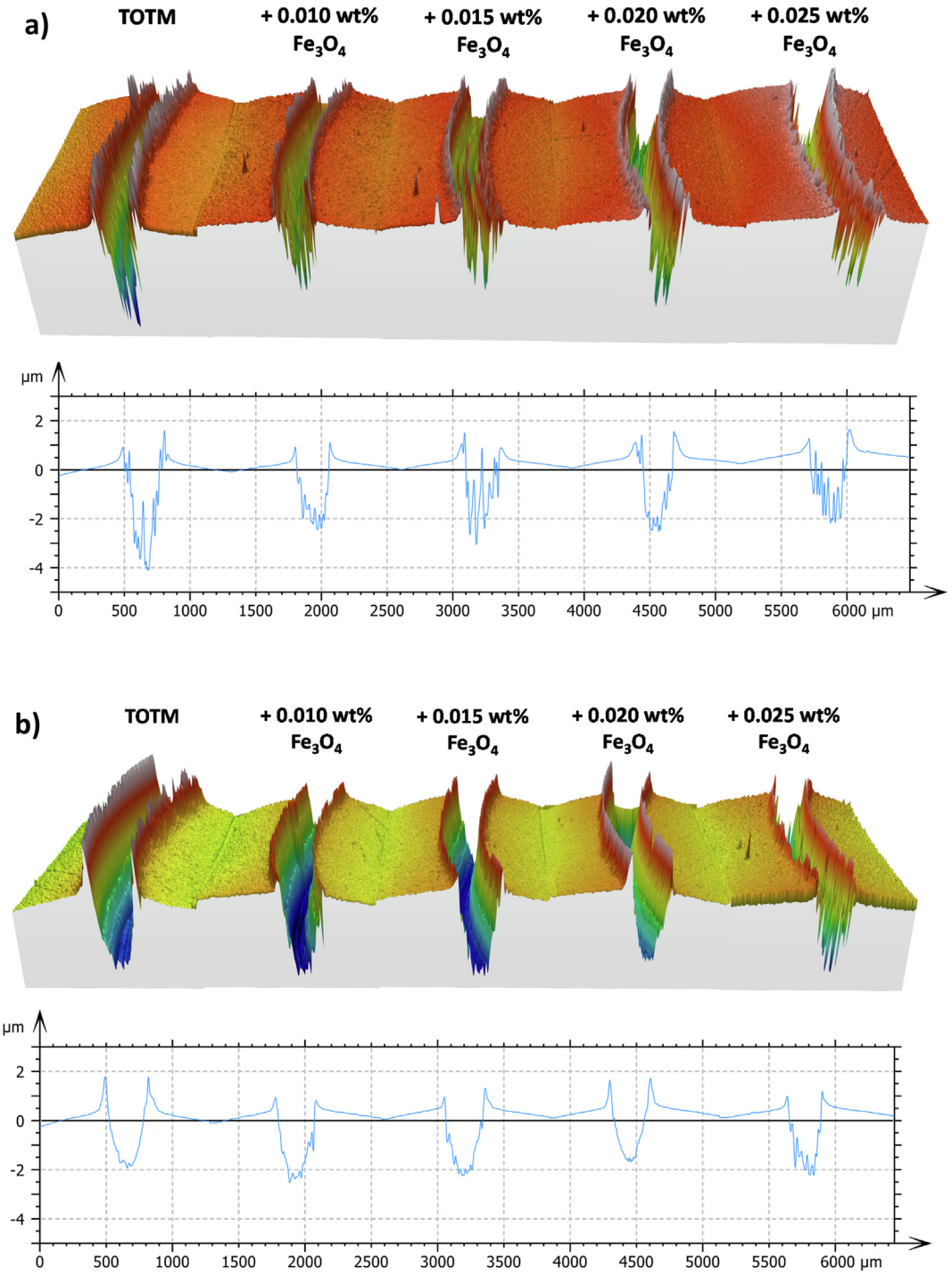

Fig. 9. 3D surface topography and cross section profiles of wear tracks produced on the steel discs for TOTM nanolubricants in a) steel-steel contact and b) silicon nitride-steel contact.

Table 4
Roughness values (Ra), and their standard deviations (σ) in worn scars on the steel discs lubricated with TOTM nanolubricants and neat TOTM for steel-steel and silicon nitride-steel contacts employing a Gaussian filter (0.08 mm cut-off).

	Steel-Steel		Silicon nitride-Steel	
Lubricant	Ra/nm	σ	Ra/nm	σ
TOTM base oil	420	41	89.5	8.2
+ 0.010 wt% Fe_3O_4-OA	200	28	88.7	9.6
+ 0.015 wt% Fe_3O_4-OA	320	30	81.4	7.5
+ 0.020 wt% Fe_3O_4-OA	220	19	44.1	4.7
+ 0.025 wt% Fe_3O_4-OA	400	31	56.7	6.2

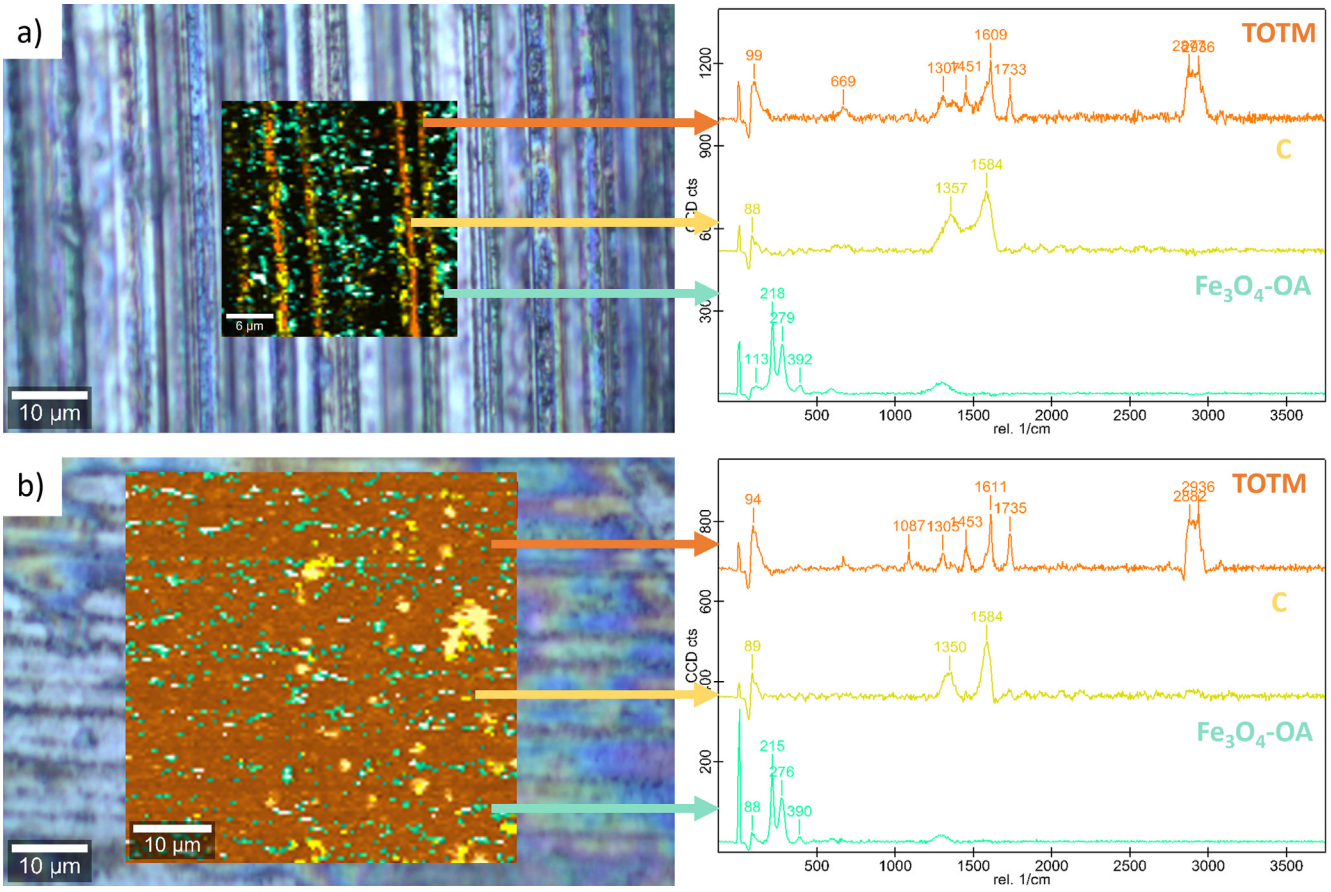

Fig. 10. Raman component mapping analysis of the wear scar of the steel disc produced at the contact a) steel-steel and b) silicon nitride-steel lubricated with TOTM + 0.025 wt% Fe_3O_4-OA.

ticles, Raman spectrum of Fe_3O_4-OA [20] shows the characteristic bands around 220, 290, 400 and 1300 cm^{-1}, which were also clearly detected (green colour) on the wear tracks in Fig. 10. In the case of steel-steel contact, an abundant deposit of TOTM and ferrite nanoparticles is observed, homogeneously distributed along the worn area of the steel disc (Fig. 10a). The grooves produced during the friction tests are clearly visible in the sliding direction along which a build-up of a tribofilm of TOTM lubricant can be seen. Raman mapping performed for the wear track generated at the steel surface of the silicon nitride-steel contact, again lubricated with the highest concentration of nanoadditive (0.025 wt %), shows that ferrite nanoparticles are also lodged along the wear track in the sliding direction but this time the base oil is observed to be spread over almost the entire surface (Fig. 10b). Hence, tribofilms formation is evidenced with the nanoadditive detection (green colour) in both tribo-pairs. However, despite these tribofilms are detected, it should be considered, as mentioned above, that in nanolubricants with high concentrations of nanoadditives, aggregation of the particles often occurs [39]. This phenomenon reduces the number of particles remaining in the contact area of the working surfaces, as the aggregates are expelled, reducing the effectiveness of the tribofilm formation [40]. In addition, some carbon flecks generated during friction tests within the wear track are unmistakably visible (yellow colour) in the steel disc of the silicon nitride-steel contact.

Taking into consideration that the worn surfaces after friction tests with Fe_3O_4-OA NPs nanolubricants are smoother than with TOTM (Table 4), and that the corresponding Raman analyses reveal the formation of tribofilms on the contact surface formed by the lubricant and the nanoadditive, it can be assumed that the improved lubricity of the base oil is due to the surface repair mechanisms and tribofilm formation played by the Fe_3O_4-OA NPs.

4. Concluding remarks

In this research work, the optimal loading of magnetic Fe_3O_4 nanoparticles coated with oleic acid in a pure TOTM lubricant was investigated to improve its tribological performance for two tribo-pairs of different material. Based on the experimental results obtained, the following conclusions can be drawn:

- The wetting ability of TOTM oil on a steel surface is improved adding Fe_3O_4-OA nanoadditives.
- All nanolubricants showed better anti-friction behaviour than the base oil, being the highest friction reduction (43%) for the for TOTM + 0.010 wt% F_3O_4-OA nanolubricant for the silicon nitride-steel contact.
- Regarding the produced wear, biggest reductions of 17% in WTW, 42% in WTD and 36% in area were reached with the TOTM + 0.010 wt% Fe_3O_4-OA nanolubricant for the steel-steel contact.
- Comparing different tribological contacts, the lowest friction coefficient was obtained in the silicon nitride-steel test, while a higher wear reduction was found in the steel-steel test.
- Roughness and Raman analyses revealed that the nanoadditives play surface repairing and tribofilm formation mechanisms.

CRediT authorship contribution statement

María J.G. Guimarey: Conceptualization, Investigation, Methodology, Writing – original draft, Writing – review & editing. **José M. Liñeira del Río:** Conceptualization, Investigation, Methodology, Writing – original draft, Writing – review & editing. **Josefa Fernández:** Supervision, Writing – review & editing.

Declaration of Competing Interest

The authors declare that they have no known competing financial interests or personal relationships that could have appeared to influence the work reported in this paper.

Acknowledgments

The following institutions and grants are acknowledged for funding this research: Government of Spain Ministry of Economy and Competitiveness (grant numbers: ENE2017-86425-C2-2-R and PID2020-112846RB-C22 projects) and Xunta de Galicia (Spain) (grant number: GRC ED431C 2020/10). Authors would like to thank the use of the RIAIDT-USC facilities, in particular to Mr. Ezequiel Vázquez. Also, to thank the NANOMAG research group for kindly providing the nanoparticles. Dr. M.J.G. Guimarey also acknowledges the Xunta de Galicia (Spain) for the postdoctoral fellowship (reference ED481B-2019-015) at Bournemouth University (UK).

References

[1] S. Boyde, Green lubricants. Environmental benefits and impacts of lubrication, Green Chem. 4 (2002) 293–307, https://doi.org/10.1039/B202272A.
[2] P. Nagendramma, S. Kaul, Development of ecofriendly/biodegradable lubricants: An overview, Renew. Sustain. Energy Rev. 16 (2012) 764–774, https://doi.org/10.1016/j.rser.2011.09.002.
[3] K. Holmberg, P. Kivikytö-Reponen, P. Härkisaari, K. Valtonen, A. Erdemir, Global energy consumption due to friction and wear in the mining industry, Tribol. Int. 115 (2017) 116–139, https://doi.org/10.1016/j.triboint.2017.05.010.
[4] M. Kalin, M. Polajnar, The Effect of Wetting and Surface Energy on the Friction and Slip in Oil-Lubricated Contacts, Tribol. Lett. 52 (2013) 185–194, https://doi.org/10.1007/s11249-013-0194-y.
[5] Y. Meng, J. Xu, Z. Jin, B. Prakash, Y. Hu, A review of recent advances in tribology, Friction 8 (2020) 221–300, https://doi.org/10.1007/s40544-020-0367-2.
[6] M. Waqas, R. Zahid, M.U. Bhutta, Z.A. Khan, A. Saeed, A Review of Friction Performance of Lubricants with Nano Additives, Materials 14 (2021), https://doi.org/10.3390/ma14216310 6310.
[7] Y.J.J. Jason, H.G. How, Y.H. Teoh, H.G. Chuah, A Study on the Tribological Performance of Nanolubricants, Processes 8 (2020), https://doi.org/10.3390/pr8111372 1372.
[8] A. Kotia, P. Rajkhowa, G.S. Rao, S.K. Ghosh, Thermophysical and tribological properties of nanolubricants: A review, Heat Mass Transf. 54 (2018) 3493–3508, https://doi.org/10.1007/s00231-018-2351-1.
[9] G. Paul, H. Hirani, T. Kuila, N.C. Murmu, Nanolubricants dispersed with graphene and its derivatives: an assessment and review of the tribological performance, Nanoscale 11 (2019) 3458–3483, https://doi.org/10.1039/C8NR08240E.
[10] W.K. Shafi, M.S. Charoo, An overall review on the tribological, thermal and rheological properties of nanolubricants, Tribol. - Mater. Surf, Interfaces 15 (2021) 20–54, https://doi.org/10.1080/17515831.2020.1785233.
[11] N.F. Azman, S. Samion, Dispersion Stability and Lubrication Mechanism of Nanolubricants: A Review, Int. J. Precis. Eng. Manuf. - Green Technol. 6 (2019) 393–414, https://doi.org/10.1007/s40684-019-00080-x.
[12] A. Singh, P. Chauhan, T.G. Mamatha, A review on tribological performance of lubricants with nanoparticles additives, Mater. Today: Proc. 25 (2020) 586–591, https://doi.org/10.1016/j.matpr.2019.07.245.
[13] Y. Chen, P. Renner, H. Liang, Dispersion of Nanoparticles in Lubricating Oil: A Critical Review, Lubricants 7 (2019), https://doi.org/10.3390/lubricants7010007 7.
[14] D. Zheng, Z.-B. Cai, M.-X. Shen, Z.-Y. Li, M.-H. Zhu, Investigation of the tribology behaviour of the graphene nanosheets as oil additives on textured alloy cast iron surface, Appl. Surf. Sci. 387 (2016) 66–75, https://doi.org/10.1016/j.apsusc.2016.06.080.
[15] N. Nunn, Z. Mahbooba, M.G. Ivanov, D.M. Ivanov, D.W. Brenner, O. Shenderova, Tribological properties of polyalphaolefin oil modified with nanocarbon additives, Diam. Relat. Mater. 54 (2015) 97–102, https://doi.org/10.1016/j.diamond.2014.09.003.
[16] Y. Chen, Y. Zhang, S. Zhang, L. Yu, P. Zhang, Z. Zhang, Preparation of Nickel-Based Nanolubricants via a Facile In Situ One-Step Route and Investigation of Their Tribological Properties, Tribol. Lett. 51 (2013) 73–83, https://doi.org/10.1007/s11249-013-0148-4.
[17] Z. Jiang, Y. Zhang, G. Yang, K. Yang, S. Zhang, L. Yu, P. Zhang, Tribological Properties of Oleylamine-Modified Ultrathin WS_2 Nanosheets as the Additive in Polyalpha Olefin Over a Wide Temperature Range, Tribol. Lett. 61 (2016), https://doi.org/10.1007/s11249-016-0643-5 24.
[18] C. Kumara, H. Luo, D.N. Leonard, H.M. Meyer, J. Qu, Organic-Modified Silver Nanoparticles as Lubricant Additives, ACS Appl. Mater. Interfaces 9 (2017) 37227–37237, https://doi.org/10.1021/acsami.7b13683.
[19] J.M. Liñeira del Río, E.R. López, F. García, J. Fernández, Tribological synergies among chemical-modified graphene oxide nanomaterials and a phosphonium ionic liquid as additives of a biolubricant, J. Mol. Liq. 336 (2021), https://doi.org/10.1016/j.molliq.2021.116885 116885.
[20] J.M. Liñeira del Río, E.R. López, M. González Gómez, S. Yáñez Vilar, Y. Piñeiro, J. Rivas, D.E.P. Gonçalves, J.H.O. Seabra, J. Fernández, Tribological Behavior of Nanolubricants Based on Coated Magnetic Nanoparticles and Trimethylolpropane Trioleate Base Oil, Nanomaterials 10 (2020), https://doi.org/10.3390/nano10040683 683.
[21] P.C. Uzoma, H. Hu, M. Khadem, O.V. Penkov, Tribology of 2D Nanomaterials: A Review, Coatings 10 (2020), https://doi.org/10.3390/coatings10090897 897.
[22] J. Sun, S. Du, Application of graphene derivatives and their nanocomposites in tribology and lubrication: a review, RSC Adv. 9 (2019) 40642–40661, https://doi.org/10.1039/C9RA05679C.
[23] W. Dai, B. Kheireddin, H. Gao, H. Liang, Roles of nanoparticles in oil lubrication, Tribol. Int. 102 (2016) 88–98, https://doi.org/10.1016/j.triboint.2016.05.020.
[24] G. Zhou, Y. Zhu, X. Wang, M. Xia, Y. Zhang, H. Ding, Sliding tribological properties of 0.45% carbon steel lubricated with Fe_3O_4 magnetic nano-particle additives in baseoil, Wear 301 (2013) 753–757, https://doi.org/10.1016/j.wear.2013.01.027.
[25] Z.S. Hu, J.X. Dong, G.X. Chen, Study on antiwear and reducing friction additive of nanometer ferric oxide, Tribol. Int. 31 (1998) 355–360, https://doi.org/10.1016/S0301-679X(98)00042-5.
[26] S. Boyde, Esters, in: L.R. Rudnick (Ed.), Synthetic, Mineral Oils and Bio-based Lubricants: Chemistry and Technology, third ed., CRC Press, Boca Raton, 2020, pp. 45–76.
[27] J.M. Liñeira del Río, M.J.G. Guimarey, M.J.P. Comuñas, J. Fernández, High pressure viscosity behaviour of tris(2-ethylhexyl) trimellitate up to 150 MPa, J. Chem. Therm. 138 (2019) 159–166, https://doi.org/10.1016/j.jct.2019.06.016.
[28] J. Fernandez, M.J. Assael, R.M. Enick, J.P.M. Trusler, International Standard for viscosity at temperatures up to 473 K and pressures below 200 MPa (IUPAC Technical Report), J. Pure Appl. Chem. 91 (2019) 161–172, https://doi.org/10.1515/pac-2018-0202.
[29] W.A. Wakeham, M.J. Assael, H.M.N.T. Avelino, S. Bair, H.O. Baled, B.A. Bamgbade, J.-P. Bazile, F.J.P. Caetano, M.J.P. Comuñas, J.-L. Daridon, J.C.F. Diogo, R.M. Enick, J.M.N.A. Fareleira, J. Fernández, M.C. Oliveira, T.V.M. Santos, C.M. Tsolakidou, In Pursuit of a High-Temperature, High-Pressure, High-Viscosity Standard: The Case of Tris(2-ethylhexyl) Trimellitate, J. Chem. Eng. Data 62 (2017) 2884–2895, https://doi.org/10.1021/acs.jced.7b00170.
[30] L.R. Rudnick, Synthetics, Mineral Oils, and Bio-Based Lubricants: Chemistry and Technology, 2020.
[31] J. Kang, M. Hadfield, R. Ahmed, The effects of material combination and surface roughness in lubricated silicon nitride/steel rolling contact fatigue, Mater. Des. 24 (2003) 1–13, https://doi.org/10.1016/S0261-3069(02)00102-4.
[32] N. Muthunilavan, G. Rajaram, Effect on lubrication regimes with silicon nitride and bearing steel balls, Tribol. Int. 116 (2017) 403–413, https://doi.org/10.1016/j.triboint.2017.06.043.
[33] S. Guan, X. Liu, Y. Zhang, Y. Liu, L. Wang, Y. Liu, Synthesis and Characterization of Polycaprolactone Modified Trimellitate Nano-Lubricant, Materials 12 (2019), https://doi.org/10.3390/ma12142273 2273.
[34] S. Qiao, Y. Shi, X. Wang, Z. Lin, Y. Jiang, Synthesis of Biolubricant Trimethylolpropane Trioleate and Its Lubricant Base Oil Properties, Energy Fuels 31 (2017) 7185–7190, https://doi.org/10.1021/acs.energyfuels.7b00876.
[35] M. Praveena, K. Guha, A. Ravishankar, S.K. Biswas, C.D. Bain, V. Jayaram, Total internal reflection Raman spectroscopy of poly(alpha-olefin) oils in a lubricated contact, RSC Adv. 4 (2014) 22205–22213, https://doi.org/10.1039/C4RA02261K.
[36] A. Panda, A.K. Sahoo, R. Kumar, R.K. Das, A review on machinability aspects for AISI 52100 bearing steel, Mater. Today: Proc. 23 (2020) 617–621, https://doi.org/10.1016/j.matpr.2019.05.422.
[37] B.A. Starkweather, X.(. Zhang, R.M. Counce, An Experimental Study of the Change in the Contact Angle of an Oil on a Solid Surface, Ind. Eng. Chem. Res. 39 (2000) 362–366, https://doi.org/10.1021/ie980693g.
[38] M.A. Coelho de Sousa Marques, M.J.G. Guimarey, V. Domínguez-Arca, A. Amigo, J. Fernández, Heat capacity, density, surface tension, and contact angle for polyalphaolefins and ester lubricants, Thermochim. Acta 703 (2021) 178994, https://doi.org/10.1016/j.tca.2021.178994.
[39] V. Zin, S. Barison, F. Agresti, L. Colla, C. Pagura, M. Fabrizio, Improved tribological and thermal properties of lubricants by graphene based nano-additives, RSC Adv. 6 (2016) 59477–59486, https://doi.org/10.1039/C6RA12029F.
[40] X. Dou, A.R. Koltonow, X. He, H.D. Jang, Q. Wang, Y.-W. Chung, J. Huang, Self-dispersed crumpled graphene balls in oil for friction and wear reduction, Proc. Natl. Acad. Sci. 113 (2016) 1528–1533, https://doi.org/10.1073/pnas.1520994113.